

See discussions, stats, and author profiles for this publication at: <https://www.researchgate.net/publication/47402934>

A New Unnatural Base Pair System between Fluorophore and Quencher Base Analogues for Nucleic Acid-Based Imaging Technology

ARTICLE *in* JOURNAL OF THE AMERICAN CHEMICAL SOCIETY · OCTOBER 2010

Impact Factor: 12.11 · DOI: 10.1021/ja1072383 · Source: PubMed

CITATIONS

22

READS

18

6 AUTHORS, INCLUDING:



Michiko Kimoto

RIKEN

63 PUBLICATIONS 1,217 CITATIONS

SEE PROFILE



Shigeyuki Yokoyama

RIKEN

760 PUBLICATIONS 21,009 CITATIONS

SEE PROFILE



Ichiro Hirao

Institute of Bioengineering and Nanotechn...

147 PUBLICATIONS 2,938 CITATIONS

SEE PROFILE

A New Unnatural Base Pair System between Fluorophore and Quencher Base Analogues for Nucleic Acid-Based Imaging Technology

Michiko Kimoto,^{†,‡} Tsuneo Mitsui,[‡] Rie Yamashige,[†] Akira Sato,[†]
Shigeyuki Yokoyama,^{†,§} and Ichiro Hirao^{*,†,‡}

*RIKEN Systems and Structural Biology Center (SSBC) and TagCyx Biotechnologies,
1-7-22 Suehiro-cho, Tsurumi-ku, Yokohama, Kanagawa 230-0045, Japan, and Department of
Biophysics and Biochemistry, Graduate School of Science, The University of Tokyo,
7-3-1 Hongo, Bunkyo-ku, Tokyo 113-0033, Japan*

Received August 12, 2010; E-mail: ihirao@riken.jp

Abstract: In the development of orthogonal extra base pairs for expanding the genetic alphabet, we created novel, unnatural base pairs between fluorophore and quencher nucleobase analogues. We found that the nucleobase analogue, 2-nitropyrrole (denoted by **Pn**), and its 4-substitutions, such as 2-nitro-4-propynylpyrrole (**Px**) and 4-[3-(6-aminohexanamido)-1-propynyl]-2-nitropyrrole (NH₂-hx-**Px**), act as fluorescence quenchers. The **Pn** and **Px** bases specifically pair with their pairing partner, 7-(2,2'-bithien-5-yl)imidazo[4,5-*b*]pyridine (**Dss**), which is strongly fluorescent. Thus, these unnatural **Dss–Pn** and **Dss–Px** base pairs function as reporter–quencher base pairs, and are complementarily incorporated into DNA by polymerase reactions as a third base pair in combination with the natural A–T and G–C pairs. Due to the static contact quenching, the **Pn** and **Px** quencher bases significantly decreased the fluorescence intensity of **Dss** by the unnatural base pairings in DNA duplexes. In addition, the **Dss–Px** pair exhibited high efficiency and selectivity in PCR amplification. Thus, this new unnatural base pair system would be suitable for detection methods of target nucleic acid sequences, and here we demonstrated the applications of the **Dss–Pn** and **Dss–Px** pairs as molecular beacons and in real-time PCR. The genetic alphabet expansion system with the replicable, unnatural fluorophore–quencher base pair will be a useful tool for sensing and diagnostic applications, as well as an imaging tool for basic research.

Introduction

Nucleic acid-based reporter probes are powerful tools for monitoring the structural changes of nucleic acids and their interactions with other molecules, as well as for detecting specific DNA sequences, as sensing and diagnostic modules.^{1,2} In particular, dual-labeled probes using fluorophore and quencher sets are widely employed as molecular beacons,^{3,4} molecular break lights,⁵ PCR primers (such as Plexor⁶ and Scorpion⁷), and PCR probes (such as TaqMan⁸ and cycling probes for

ICAN⁹ (isothermal and chimeric primer-initiated amplification of nucleic acids). Thus, pursuing new types of highly sensitive fluorophore and quencher sets is one of the important issues for advancing imaging biotechnologies.

Conventional fluorophore and quencher sets for nucleic acid-based reporter probes are designed by linking fluorophore and quencher molecules to pairing base moieties or into proximate oligonucleotides. The fluorescence intensity is reduced by the quencher partner via fluorescence resonance energy transfer (FRET) or static quenching.¹⁰ Static quenching occurs through the direct contact between the fluorophore and quencher molecules and is more efficient than FRET-type quenching. For example, in a molecular beacon,³ the fluorophore EDANS, at the 5'-terminus of the hairpin stem region, is effectively quenched by the direct hydrophobic interaction with the quencher DABCYL, at the 3'-terminus. By hybridizing with a complementary nucleic acid target, the fluorophore moves away from the quencher, allowing the visible detection of the fluorescence in a test tube.

Another attractive idea for the incorporation of fluorophore and quencher sets into nucleic acid probes is the creation of artificial extra base pairs (unnatural base pairs) toward the

[†] RIKEN Systems and Structural Biology Center (SSBC).

[‡] TagCyx Biotechnologies.

[§] The University of Tokyo.

- (1) Marras, S. A. *Methods Mol. Biol.* **2006**, 335, 3.
- (2) Marras, S. A. *Mol. Biotechnol.* **2008**, 38, 247.
- (3) Tyagi, S.; Kramer, F. R. *Nat. Biotechnol.* **1996**, 14, 303.
- (4) Yang, C. J.; Medley, C. D.; Tan, W. *Curr. Pharm. Biotechnol.* **2005**, 6, 445.
- (5) Biggins, J. B.; Prudent, J. R.; Marshall, D. J.; Ruppen, M.; Thorson, J. S. *Proc. Natl. Acad. Sci. U.S.A.* **2000**, 97, 13537.
- (6) Sherrill, C. B.; Marshall, D. J.; Moser, M. J.; Larsen, C. A.; Daude-Snow, L.; Jurczyk, S.; Shapiro, G.; Prudent, J. R. *J. Am. Chem. Soc.* **2004**, 126, 4550.
- (7) Whitcombe, D.; Theaker, J.; Guy, S. P.; Brown, T.; Little, S. *Nat. Biotechnol.* **1999**, 17, 804.
- (8) Livak, K. J.; Flood, S. J.; Marmaro, J.; Giusti, W.; Deetz, K. *PCR Methods Appl.* **1995**, 4, 357.
- (9) Uemori, T.; Mukai, H.; Takeda, O.; Moriyama, M.; Sato, Y.; Hokazono, S.; Takatsu, N.; Asada, K.; Kato, I. *J. Biochem.* **2007**, 142, 283.
- (10) Johansson, M. K. *Methods Mol. Biol.* **2006**, 335, 17.

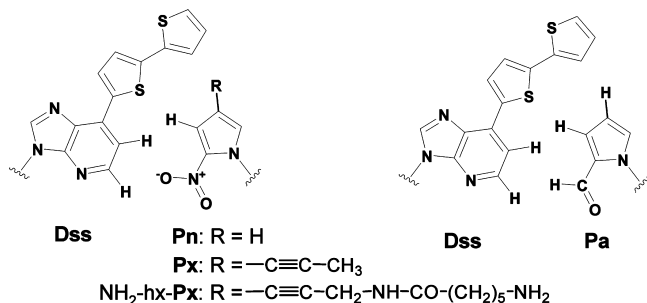


Figure 1. The unnatural **Dss–Pn**, **Dss–Px**, and **Dss–Pa** pairs.

expansion of the genetic alphabet. Several new base pairs that exhibit high fidelity in replication and transcription have been developed.^{11–19} In addition, many fluorescent base analogues have been synthesized.^{20–25} Among them, we recently developed a fluorescent base analogue, 7-(2,2'-bithien-5-yl)-imidazo[4,5-*b*]pyridine (**Dss**),²⁶ which exhibits a strong fluorescence emission centered at 456 nm, upon excitation at 385 nm, in oligonucleotides. **Dss** was developed to improve the fluorescence properties of our previously designed unnatural **Ds** (7-(2-thienyl)-imidazo[4,5-*b*]pyridine)¹⁹ base. **Ds** specifically pairs with **Pa**,¹⁹ 2-nitropyrrrole (**Pn**)²⁷ or 2-nitro-4-propynylpyrrole (**Px**)¹⁶ in replication and transcription (Figure 1). The **Dss** base also functions as an unnatural base pair with its pairing partner **Pa** in replication and transcription.²⁶ However, at this point, no quencher base analogues for an unnatural base pair system have been reported.

Here we present the first fluorophore–quencher base pair and demonstrate its function in polymerase reactions. In the study of **Dss** with other pairing partners besides **Pa**, such as **Pn** and **Px**, we unexpectedly found that the fluorescence of **Dss** was strongly quenched by the pairing with **Pn** or **Px** in a DNA duplex. The **Pn** and its 4-substitutions, such as **Px** and 4-[3-(6-aminohexanamido)-1-propynyl]-2-nitropyrrrole (**NH₂-hx-Px**), have remarkable abilities as quencher molecules. In addition, the **Dss–Pn** and **Dss–Px** pairs function as an extra, third base pair in replication, with high pairing selectivity. The 2'-deoxyribonucleoside 5'-triphosphates of **Dss** and **Pn** were both site specifically incorporated into DNA opposite each other by replication. In particular, the **Dss–Px** pair exhibited high

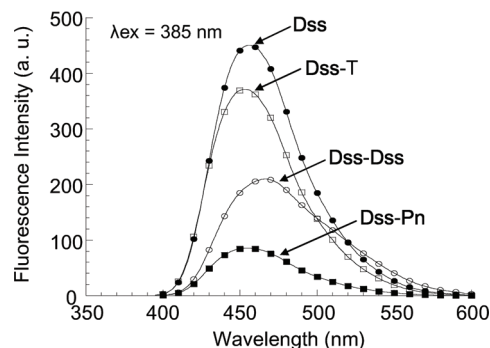
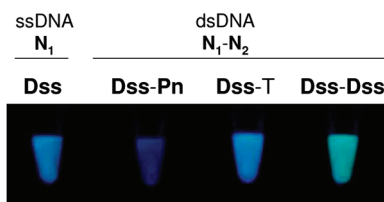
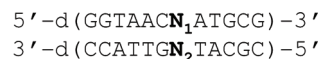


Figure 2. Fluorescence quenching of **Dss** by **Pn** in a double-stranded DNA fragment. For visible detection, single-stranded or double-stranded DNA fragments (12-mer, 5 μM) were illuminated at 365 nm, in a buffer containing 10 mM sodium phosphate (pH 7.0), 100 mM NaCl, and 0.1 mM EDTA. The fluorescence emission spectra of each DNA oligomer (5 μM) were measured with excitation at 385 nm at 25 $^{\circ}\text{C}$, in 10 mM sodium phosphate (pH 7.0) buffer, containing 100 mM NaCl and 0.1 mM EDTA. **Dss** indicates a single-stranded 12-mer containing one **Dss** base. **Dss–Pn**, **Dss–T**, and **Dss–Dss** indicate double-stranded 12-mers containing one **Dss–Pn**, **Dss–T**, and **Dss–Dss** pair, respectively.

efficiency and selectivity in PCR amplification. By using the **Dss–Pn** and **Dss–Px** pair systems, we demonstrated their abilities as a molecular beacon and in real-time PCR to detect nucleic acid targets with a specific sequence. Thus, this contact quenching system composed of the unnatural base pairs between the fluorophore and quencher base analogues is applicable to replication and transcription.

Results

Quenching of the Dss Fluorescence by Base Pairing with Pn. During our studies of the unnatural **Dss** and **Pn** base pair, we found that the fluorescence intensity of **Dss** was significantly reduced by base pairing with **Pn** in a DNA duplex. As shown in Figure 2, the strong fluorescence of **Dss** in a DNA 12-mer was quenched by hybridization with its complementary 12-mer strand containing **Pn**. Hybridization with other 12-mers containing **T** or **Dss**, in place of **Pn**, did not quench the **Dss** fluorescence. The thermal stability of the 12-mer duplex containing the **Dss–Pn** pair ($T_m = 45.4$ $^{\circ}\text{C}$ in a buffer containing 100 mM NaCl, 10 mM sodium phosphate (pH 7.0), and 0.1 mM EDTA) was higher than that containing **Dss–T** ($T_m = 43.9$ $^{\circ}\text{C}$); both fragments formed the duplex under the fluorescence experiment conditions at room temperature.

To confirm the quenching ability of the **Pn** base, we examined the steady-state fluorescence quenching of the 2'-deoxyribonucleoside 5'-triphosphate of **Dss** (**dDssTP**), in the presence of **dPnTP** or the natural base triphosphates, at 25 $^{\circ}\text{C}$ (Figure 3). The fluorescence of **dDssTP** (5 μM) was quenched more than 10-fold in the presence of **dPnTP** (1905 μM), and its Stern–Volmer constant (K_{SV}) was $4.9 \times 10^3 \text{ M}^{-1}$, which is much larger than that of the well-known guanine quenching ($K_{SV} = 52 \text{ M}^{-1}$

- (11) Krueger, A. T.; Kool, E. T. *Curr. Opin. Chem. Biol.* **2007**, *11*, 588.
- (12) Krueger, A. T.; Kool, E. T. *Chem. Biol.* **2009**, *16*, 242.
- (13) Henry, A. A.; Romesberg, F. E. *Curr. Opin. Chem. Biol.* **2003**, *7*, 727.
- (14) Benner, S. A. *Acc. Chem. Res.* **2004**, *37*, 784.
- (15) Hirao, I. *Curr. Opin. Chem. Biol.* **2006**, *10*, 622.
- (16) Kimoto, M.; Kawai, R.; Mitsui, T.; Yokoyama, S.; Hirao, I. *Nucleic Acids Res.* **2009**, *37*, e14.
- (17) Malyshev, D. A.; Seo, Y. J.; Ordoukhanian, P.; Romesberg, F. E. *J. Am. Chem. Soc.* **2009**, *131*, 14620.
- (18) Yang, Z.; Chen, F.; Chamberlin, S. G.; Benner, S. A. *Angew. Chem., Int. Ed.* **2010**, *49*, 177.
- (19) Hirao, I.; Kimoto, M.; Mitsui, T.; Fujiwara, T.; Kawai, R.; Sato, A.; Harada, Y.; Yokoyama, S. *Nat. Methods* **2006**, *3*, 729.
- (20) Wilson, J. N.; Kool, E. T. *Org. Biomol. Chem.* **2006**, *4*, 4265.
- (21) Sinkeldam, R. W.; Greco, N. J.; Tor, Y. *Chem. Rev.* **2010**, *110*, 2579.
- (22) Cremona, C. R. *Methods Enzymol.* **2003**, *360*, 128.
- (23) Hawkins, M. E. *Cell Biochem. Biophys.* **2001**, *34*, 257.
- (24) Hikida, Y.; Kimoto, M.; Yokoyama, S.; Hirao, I. *Nat. Protoc.* **2010**, *5*, 1312.
- (25) Kimoto, M.; Mitsui, T.; Harada, Y.; Sato, A.; Yokoyama, S.; Hirao, I. *Nucleic Acids Res.* **2007**, *35*, 5360.
- (26) Kimoto, M.; Mitsui, T.; Yokoyama, S.; Hirao, I. *J. Am. Chem. Soc.* **2010**, *132*, 4988.
- (27) Hirao, I.; Mitsui, T.; Kimoto, M.; Yokoyama, S. *J. Am. Chem. Soc.* **2007**, *129*, 15549.

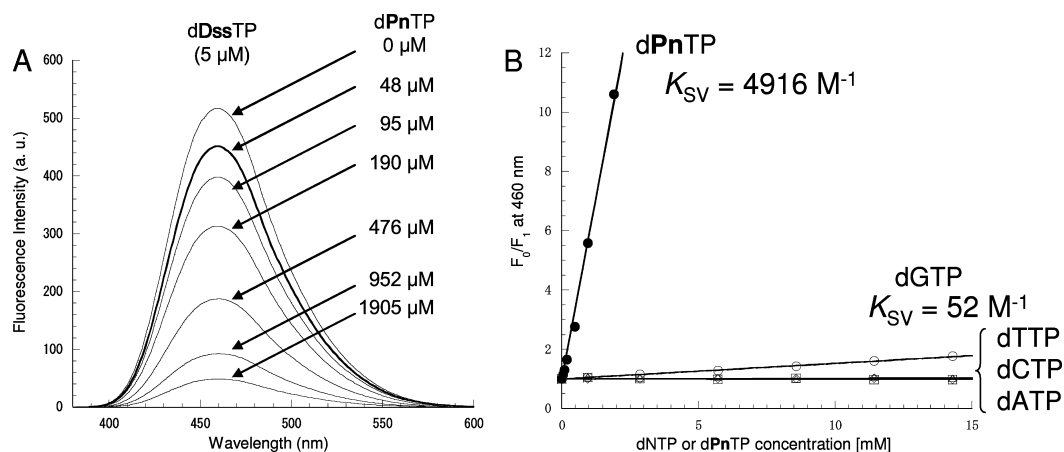


Figure 3. Steady-state fluorescence emission spectra of dDssTP (5 μM) in the presence of dPnTP (0–1905 μM) (A) and Stern–Volmer plots for fluorescence quenching of dDssTP by dPnTP, dATP, dGTP, dCTP, or dTTP (B). The solutions were irradiated at 370 nm in 10 mM sodium phosphate (pH 7.0) buffer, containing 100 mM NaCl and 0.1 mM EDTA, at 20 °C. The fluorescence intensity (F_0) of the dDssTP solution (5 μM), divided by the fluorescence intensity in the presence of various concentrations of dPnTP, dATP, dGTP, dCTP, or dTTP (F), was plotted against each triphosphate concentration.

for dGTP). There was no significant difference in the shape of the emission spectra of dDssTP during quenching with dPnTP, indicating the absence of a specific physical interaction between dDssTP and dPnTP in the solution. We also examined the quenching abilities of 2'-deoxyribonucleosides of Pn derivatives and related compounds with the 2'-deoxyribonucleoside of fluorescent Dss (see Supporting Information). The quenching efficiency of Px was higher than that of Pn, suggesting that the quenching ability of 2-nitropyrrole is augmented by increasing its conjugated unsaturation. 3-Nitropyrrole, which is well-known as a universal base,^{28,29} showed less quenching as compared to that of Pn. In addition, Pa lacked quenching ability.

The quenching of the Dss fluorescence by Pn was also examined by the fluorescence change during the thermal denaturation of a hairpin DNA containing the Dss–Pn pair in the stem region (Figure 4). We chemically synthesized the tetraloop hairpin (34-mer), in which the Dss–Pn pair was incorporated into the middle of the 10-bp stem region. The Dss fluorescence of the hairpin DNA was monitored while the temperature was increased. The melting curve of the hairpin structure was observed by the Dss fluorescence change, while that of a single-stranded DNA fragment (12-mer) containing Dss showed a slight decrease. The Dss fluorescence recovered at around 60 °C, indicating that the quenching by the Pn pairing was relieved upon the denaturation of the hairpin structure.

Specific Dss–Pn Pairing in Replication by the Klenow Fragment. The Dss base efficiently and selectively pairs with the Pn base in replication, and both unnatural base substrates were complementarily incorporated into DNA by polymerases. We first examined the efficiency and selectivity of the Dss–Pn pairing by single-nucleotide insertion experiments,^{30–32} using the exonuclease-deficient Klenow fragment of *Escherichia coli* DNA polymerase I (Table 1). The kinetic parameters of the incorporation efficiency of the Dss–Pn pairing were compared with those of other cognate pairings, Dss–Pa²⁶ and A–T, as

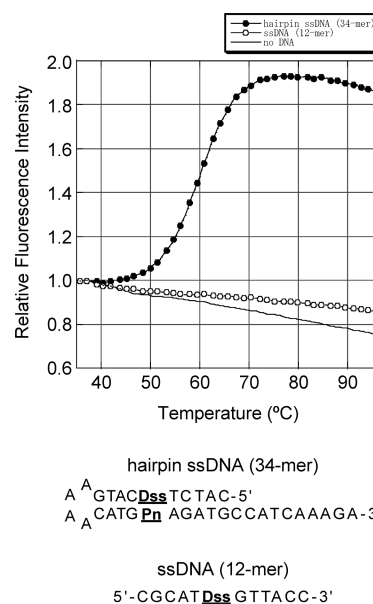


Figure 4. Melting curves obtained by the fluorescence intensity changes of the hairpin fragment containing the Dss–Pn pair. Fluorescence intensities of the hairpin DNA containing the Dss–Pn pair (34-mer) or a single-stranded DNA containing Dss (12-mer) (1 μM each) were measured in 1× ExTaq buffer (TaKaRa), containing the 1000-fold diluted ROX dye as a reference. The fluorescence was measured with ALEXA Fluor 350 and ROX/Texas Red filter sets on an Mx3005P system (Stratagene). The relative fluorescence intensity (ALEXA/ROX) at each temperature was normalized by dividing it by that obtained at 35 °C.

well as the noncognate pairings between the unnatural and natural bases. The incorporation efficiency of the Dss–Pn pairing (Table 1, entries 1 and 12) was improved 2–3-fold relative to that of the Dss–Pa pairing (Table 1, entries 2 and 13). In addition, the Dss base in the templates efficiently prevented the misincorporation of the natural base substrates (Table 1, entries 3–6). The misincorporation of the natural base substrates opposite Pn (Table 1, entries 14–17) was also less efficient than the incorporation of dDssTP opposite Pn, and the efficiency of the highest misincorporation, dGTP opposite Pn (Table 1, entry 15), was 527-fold lower than that of the dDssTP incorporation opposite Pn. The misincorporation of dPnTP opposite the natural bases was >200-fold less efficient than the dTTP incorporation opposite A. Therefore, the natural base

(28) Nichols, R.; Andrews, P. C.; Zhang, P.; Bergstrom, D. E. *Nature* **1994**, *369*, 492.

(29) Loakes, D.; Brown, D. M.; Linde, S.; Hill, F. *Nucleic Acids Res.* **1995**, *23*, 2361.

(30) Petruska, J.; Goodman, M. F.; Boosalis, M. S.; Sowers, L. C.; Cheong, C.; Tinoco, I., Jr. *Proc. Natl. Acad. Sci. U.S.A.* **1988**, *85*, 6252.

(31) Goodman, M. F.; Creighton, S.; Bloom, L. B.; Petruska, J. *Crit. Rev. Biochem. Mol. Biol.* **1993**, *28*, 83.

(32) Kimoto, M.; Yokoyama, S.; Hirao, I. *Biotechnol. Lett.* **2004**, *26*, 999.

Table 1. Steady-State Kinetics of Single-Nucleotide Insertion of the Cognate and Noncognate Pairings Involving **Dss** and **Pn** in Replication^a

For Entries 1-11

Primer 5'-FAM-ACTCACTATAGGGAGGAAGA

Template 3'-TATTATGCTGAGTGATATCCCTCCTTCT**NT**CTCGA

For Entries 12-22

Primer 5'-FAM-ACTCACTATAGGGAGCTTCT

Template 3'-TATTATGCTGAGTGATATCCCTCGAAGAN**AG**AGCT

entry	template base (N)	nucleoside triphosphate	K_M (μ M)	k_{cat} (min^{-1})	k_{cat}/K_M ($\text{min}^{-1} \text{M}^{-1}$)
1	Dss	d Pn TP	100 (20) ^b	29 (7)	2.9×10^5
2 ^d	Dss	d Pa TP	150 (50)	15 (3)	1.0×10^5
3 ^d	Dss	dATP	n.d. ^c	n.d.	—
4 ^d	Dss	dGTP	n.d.	n.d.	—
5 ^d	Dss	dCTP	n.d.	n.d.	—
6 ^d	Dss	dTTP	n.d.	n.d.	—
7 ^e	A	d Pn TP	130 (60)	6.7 (3.0)	5.2×10^4
8 ^e	G	d Pn TP	80 (56)	2.9 (1.0)	3.6×10^4
9 ^e	C	d Pn TP	140 (130)	0.26 (0.12)	1.9×10^3
10 ^e	T	d Pn TP	140 (40)	7.2 (1.5)	5.1×10^4
11	A	dTTP	0.7 (0.4)	7.0 (3.7)	1.0×10^7
12	Pn	d Dss TP	0.77 (0.2)	22 (8)	2.9×10^7
13 ^d	Pa	d Dss TP	1.3 (0.6)	21 (6)	1.6×10^7
14 ^e	Pn	dATP	510 (210)	7.0 (4.1)	1.4×10^4
15 ^e	Pn	dGTP	220 (30)	12 (3)	5.5×10^4
16 ^e	Pn	dCTP	n.d.	n.d.	—
17 ^e	Pn	dTTP	630 (80)	3.3 (1.0)	5.2×10^3
18 ^d	A	d Dss TP	5.0 (2.4)	1.8 (0.3)	3.6×10^5
19 ^d	G	d Dss TP	3.6 (0.2)	2.3 (0.1)	6.4×10^5
20 ^d	C	d Dss TP	7.5 (1.8)	2.6 (0.5)	3.5×10^5
21 ^d	T	d Dss TP	6.2 (0.1)	5.5 (0.4)	8.9×10^5
22	T	dATP	0.8 (0.4)	8.3 (4.6)	1.0×10^7

^a Determined at 37 °C for 1–4 min, using 5 μ M template–primer duplex, 3–20 nM KF (exo[−]), and 0.15–600 μ M nucleoside triphosphate in a solution (10 μ L) containing 50 mM Tris-HCl (pH 7.5), 10 mM MgCl₂, 1 mM DTT, and 0.05 mg/mL bovine serum albumin. Each parameter was averaged from five data sets. ^b Standard deviations are given in parentheses. ^c The reaction was too slow to calculate the parameters ($k_{cat} < 0.013$). ^d Reference 26. ^e Reference 27.

substrates could predominantly be incorporated into DNA opposite the complementary natural base partners, even in the presence of d**Pn**TP. In contrast, the misincorporation efficiency of d**Dss**TP opposite the natural bases was relatively high and was only 11–29-fold lower than that of dATP incorporation opposite T. However, the d**Dss**TP incorporation opposite **Pn** also exhibited superior efficiency, and was 2.9-fold higher than that of dATP incorporation opposite T. Thus, the undesired **Dss** misincorporation opposite the natural bases could be addressed by adjusting each substrate concentration. For high fidelity replication, decreasing the concentration of d**Dss**TP, relative to those of the natural base substrates, accomplished faithful replication, as described below.

Next, we examined the primer extension of the **Dss–Pn** pairing, using the **Pn**-containing 35-mer template, the 5'-³²P-labeled 23-mer primer, and the substrates, d**Dss**TP, dCTP, and dTTP, with the exonuclease-proficient Klenow fragment (Figure 5). For the primer extension, we added only dCTP and dTTP as natural base substrates, and thus, the labeled 33-mer will be obtained as the full-length product by faithful extension. As we observed in the **Dss–Pa** pair experiments,²⁶ the presence of equal amounts of d**Dss**TP and the natural base substrates inhibited the further extension after the d**Dss**TP incorporation opposite **Pn** at position 29. However, by a 20-fold decrease of the d**Dss**TP concentration relative to those of the natural base substrates, the primer extension efficiently occurred in the presence of 0.5 μ M d**Dss**TP and 10 μ M dCTP and dTTP. Reducing the d**Dss**TP concentration, relative to those of the natural base substrates, is desirable for faithful replication involving the **Dss–Pn** pairing, because the misincorporation

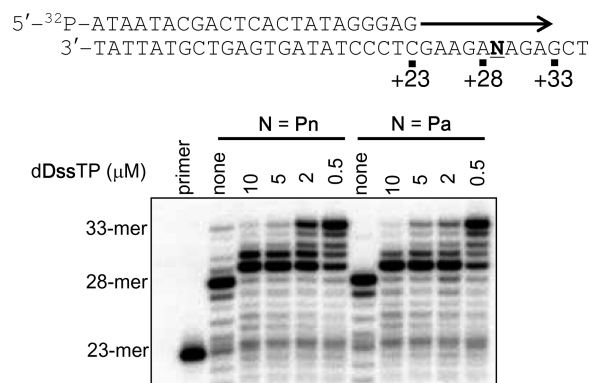


Figure 5. Primer extension involving the **Dss** incorporation opposite **Pn** or **Pa** by the exonuclease-proficient Klenow fragment. Extension was performed at 37 °C for 3 min, using the enzyme (1 unit), the primer–template duplex (200 nM), d**Dss**TP (0–10 μ M), dCTP (10 μ M), and dTTP (10 μ M), in a buffer containing 10 mM Tris-HCl (pH 7.5), 7 mM MgCl₂, and 0.1 mM DTT.

of d**Dss**TP opposite the natural bases was relatively high, as described above. The primer extension completely stopped at position 33, indicating that d**Dss**TP was not misincorporated opposite C.

PCR Amplification Involving the **Dss–Px Pair.** The **Dss–Px** pair also functions in PCR amplification with high efficiency and selectivity. In our previous studies on the unnatural **Ds–Px** base pair, increasing the hydrophobicity of **Pn** by attaching a propynyl group, as shown in **Px**, improved its incorporation efficiency into DNA opposite **Ds** in replication.¹⁶ Thus, as the

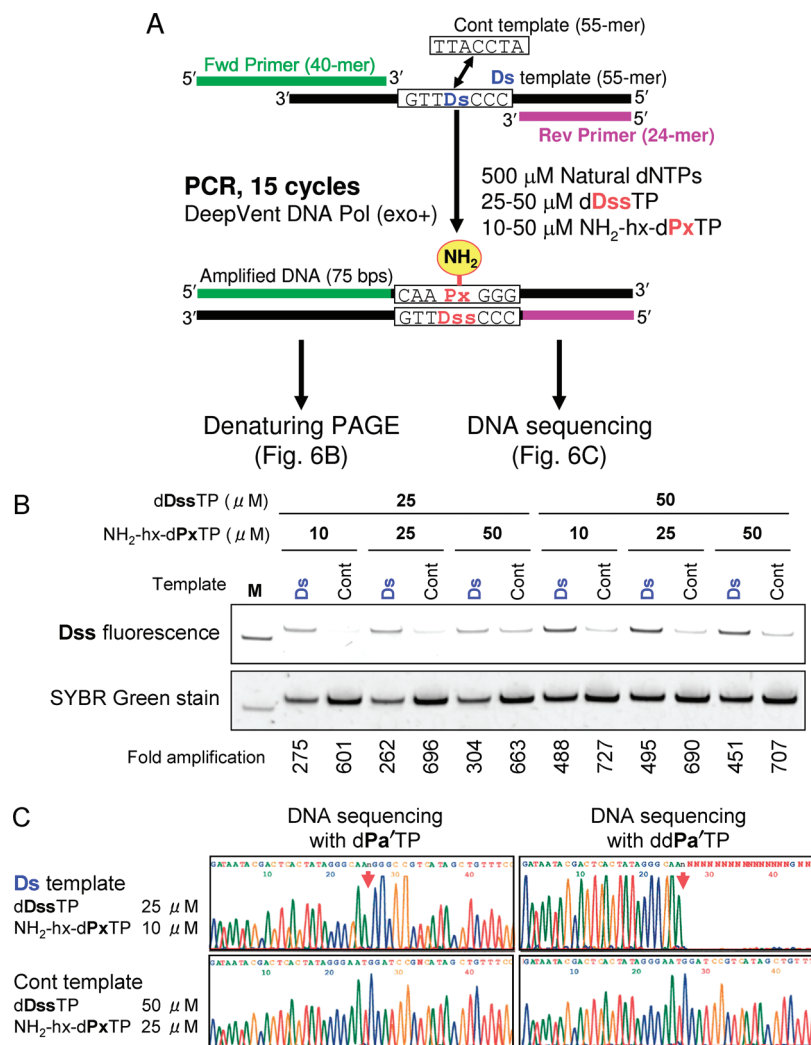


Figure 6. PCR amplification involving the **Dss** and **NH₂-hx-Px** pair. (A) Scheme for PCR amplification in the presence of **dDssTP** and **NH₂-hx-dPxTP** with DeepVent DNA polymerase, using a DNA template containing **Ds** (55-mer) and primers (40-mer and 25-mer). (B) Polyacrylamide-gel analysis of the DNA fragments (75 bps) amplified by 15 cycles of PCR. The amplified DNAs were detected by the fluorescence of the incorporated **Dss** base (upper gel) and by SYBR Green staining of the products (lower gel). M (marker) indicates a biotin-labeled, single-stranded DNA (61-mer) containing one **Dss**. (C) Sequencing of the 15-cycle amplified DNA fragments using the **Ds** template and a control template composed of only the natural bases (55-mer), in the presence of **dPa'TP** (50 μM) or **ddPa'TP** (50 μM). The arrows indicate the unnatural base positions.

pairing partner of **Dss** in PCR amplification, the **Px** substrate might be more favorable than the **Pn** substrate. We performed PCR amplification in the presence of a substrate mixture with different concentrations of **dDssTP** (25 or 50 μM), **NH₂-hx-dPxTP** (10, 25, or 50 μM), and the natural base substrates (500 μM each), using the exonuclease-proficient DeepVent DNA polymerase (Figure 6A). As the initial input DNA, we used a single-stranded DNA fragment (25 fmol) containing **Ds**. For this template, the unnatural base pair with **Dss** and **NH₂-hx-Px** would be incorporated at the initial **Ds** position in the PCR-amplified, double-stranded DNA fragments.

After 15 cycles of PCR, the initial DNA was amplified, and **Dss** and **NH₂-hx-Px** were complementarily incorporated into the amplified DNA. The amplified products were analyzed on a denaturing polyacrylamide gel by two methods: **Dss** fluorescence detection and SYBR Green staining (Figure 6B). The unnatural base pair incorporation was detected by **Dss** fluorescence in the amplified DNA, and the PCR amplification efficiency was determined by SYBR Green staining. The highly selective **Dss-Px** pairing in PCR was achieved by decreasing the concentrations of the unnatural base substrates (25 μM

dDssTP and 10 μM **NH₂-hx-dPxTP**). Although the amplification efficiency (275-fold amplification after 15 cycles of PCR) was decreased by half, as compared to that (601-fold amplification) of the control amplification of the natural base template (Control template), lower concentrations of the unnatural base substrates reduced the misincorporation of unnatural base substrates opposite the natural bases in the templates. By increasing the **dDssTP** and **NH₂-hx-dPxTP** concentrations, the **Dss** fluorescence was also observed from the amplified DNA of the Control template. In PCR with 25 μM **dDssTP** and 10 μM **NH₂-hx-dPxTP**, the misincorporation was reduced to less than 0.1% per natural base position in the 75-mer amplified products. Since the amplified double-stranded DNA fragments containing the **Dss-Px** pair were denatured on the gel containing 7 M urea, the **Dss** fluorescence of the fragments could be detected without quenching by **Px**. Upon pairing with **Px**, the **Dss** fluorescence in the duplex was significantly reduced on a native gel (data not shown).

The high selectivity of the **Dss-Px** pairing in PCR and the incorporation position were confirmed by DNA sequencing of the PCR products (Figure 6C). The DNA sequencing involving

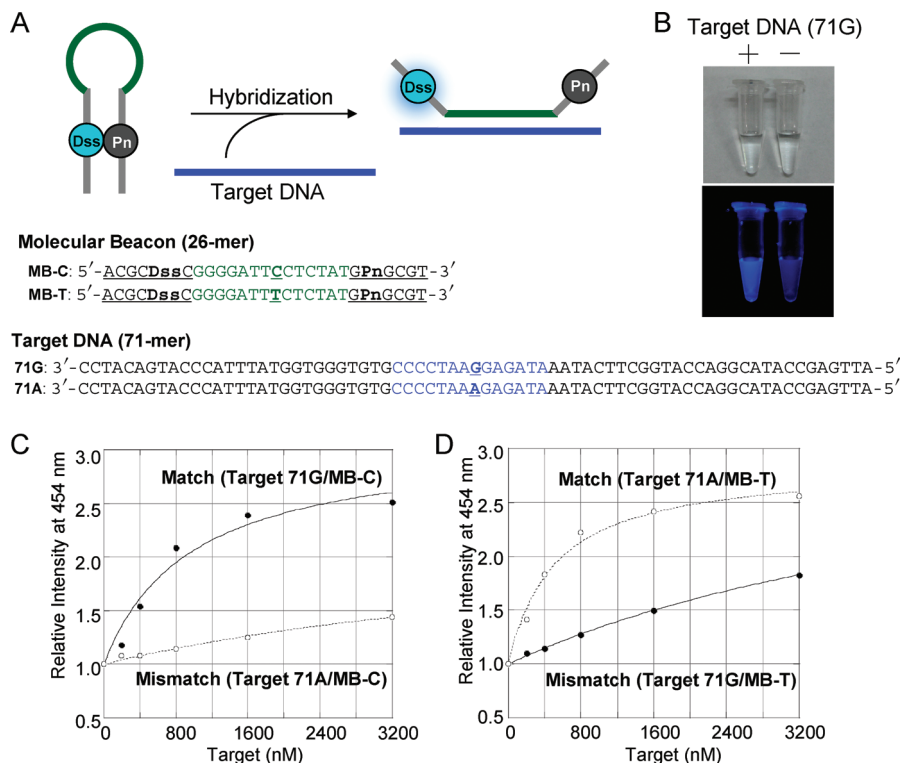


Figure 7. Scheme for a target DNA detection system, using molecular beacons containing the **Dss–Pn** pair (A). Visible **Dss** fluorescence of molecular beacons by hybridization to its target DNA (B). After the annealing of the molecular beacon MB-C (1 μ M) with or without a target DNA fragment, 71G, (1 μ M), in a solution containing 10 mM sodium phosphate (pH 7.0), 100 mM NaCl, and 0.1 mM EDTA, the **Dss** fluorescence was observed by illumination at 365 nm (lower picture) at room temperature. Detection of target DNA sequences with one base difference (71G and 71A), using molecular beacons MB-C (C) and MB-T (D). The molecular beacons (400 nM) were mixed with the target DNA fragments (71G or 71A, 0–3200 nM), and the **Dss** fluorescence was directly measured at 45 $^{\circ}$ C, with excitation at 390 nm and emission at 454 nm.

the unnatural base pair was performed by the conventional dideoxy-dye terminator method, in the presence of an unnatural base substrate (**dPa**'TP) or the dideoxyribonucleoside substrate of the unnatural base (**ddPa**'TP).^{16,19,27} In the sequencing in the presence of **dPa**'TP, the unnatural base position was observed as a gap, and we confirmed that the **Dss–Px** pair was inserted at the initial **Ds** position of the template by PCR amplification. From the sequencing in the presence of **ddPa**'TP, we estimated the fidelity-per-cycle^{16,19} of the **Dss–Px** pairing in PCR, which was more than 99.5% per PCR cycle. In the sequencing, **ddPa**'TP was incorporated into the sequencing strand opposite **Dss** in the PCR products, and the sequencing reaction was almost completely terminated at the unnatural base position. If the unnatural base position was replaced with the natural base during PCR, then the sequencing peaks after the unnatural base position appeared in the sequencing with **ddPa**'TP.

Molecular Beacon Containing the **Dss–Pn pair.** We applied the **Dss–Pn** pair as a molecular beacon³ for the highly sensitive detection of a target DNA sequence. The **Dss–Pn** pair was introduced into the stem region with six base pairs of molecular beacons (MB-C and MB-T, 26-mer) containing a 14-base single-stranded loop, which comprises the complementary sequence to a single-stranded target DNA (Figure 7A). The **Dss** fluorescence of the beacons alone was almost quenched by the pairing between **Dss** and **Pn** in the stem region. MB-C (1 μ M) was mixed with an equal amount of the target DNA (71G, 71-mer), which has the complementary sequence, in 10 mM phosphate buffer (pH 7.0) containing 100 mM NaCl, and 0.1 mM EDTA. After the solution was subjected to the annealing process, the

fluorescence was observed with the naked eye by 375 nm excitation at room temperature (Figure 7B).

A single base difference in the target DNA was recognized by the beacons. Each beacon (400 nM), MB-C or MB-T, which has one base difference between each other in the loop sequence, was incubated with 0–3200 nM target DNA, 71G or 71A, in the 100 mM NaCl solution at 45 $^{\circ}$ C for 5 min. Without the annealing process, the fluorescence intensity of each set of the beacon and the target DNA was monitored by emission at 454 nm after excitation at 390 nm. The correct sets, MB-C and 71G, and MB-T and 71A, exhibited high emission relative to those of the mismatched sets, MB-C and 71A, and MB-T and 71G (C and D of Figure 7).

Real-Time PCR Using the **Dss–Px Pair.** The **Dss–Px** pair was employed for real-time quantitative PCR by using a **Px** substrate, **NH₂-hx-dPxTP**, and a PCR primer containing an extra tag with **Dss**. In the system, real-time qPCR was achieved by monitoring the reduction of the **Dss** fluorescence, by the incorporation of the **Px** quencher opposite **Dss** in the primer during amplification (Figure 8A). For the system, we used Titanium Taq DNA polymerase, which lacks 3'–5' exonuclease activity but exhibits unidirectional high efficiency and selectivity for the **Px** incorporation opposite **Dss**. To reduce the production of primer dimers during PCR, we employed a two-step cycle, including 95 $^{\circ}$ C for denaturing the double-stranded DNA and 68 $^{\circ}$ C for annealing and elongation. Plots B and C of Figure 8 show the amplification and Ct values plots for 30,000, 15,000, 3,000, 1500, 300, 150, 30, 15, and 3 copies of the target DNA fragments, respectively. Although the Ct values for the 3 initial copies of the

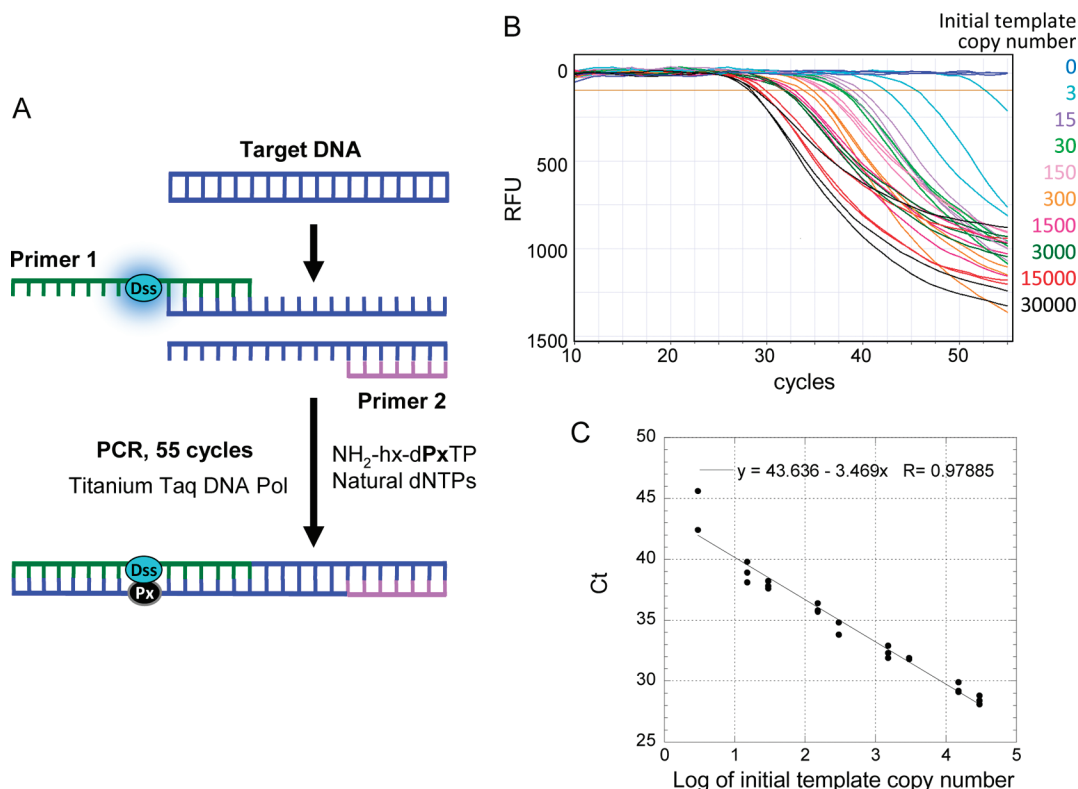


Figure 8. Quantitative real-time PCR using the **Dss**–**Px** pair amplification system. (A) Scheme of the real-time PCR system, using a primer containing a **Dss** tag, **NH₂-hx-dPxTP**, and Titanium Taq DNA polymerase. (B) Amplification plots of 55 cycles of PCR, using 0–30,000 copies of the initial target DNA fragment. The **Dss** fluorescence was detected by ALEXA Fluor 350 (350–440 nm), using an Mx3005P system (Stratagene). (C) Standard curve for the **Dss**–**Px** pair amplification system. Ct values were plotted against the logarithm of DNA copy number (log *N*). The equation for the regression line is indicated with the correlation coefficient (*R*).

target DNA showed some variation, the system indicated the high linearity in a dynamic range from 15 to 30,000 copies for qPCR.

Discussion

We developed a unique, unnatural base pair system comprising the set of a fluorophore base analogue, **Dss**, and a quencher base analogue, **Pn** or 4-substituted **Pn** bases, such as **Px** and **NH₂-hx-Px**, for the expansion of the genetic alphabet. The 2-nitropyrrole moiety of **Pn** and **Px** exhibits high quenching ability, and the strong fluorescence of its pairing partner **Dss** is efficiently reduced by the contact quenching through the base pairing with **Pn** or **Px**. The **Dss**–**Pn** and **Dss**–**Px** pairs function in replication as a third base pair between hydrophobic unnatural bases, which were designed by extended shape-complementarity. The shape of **Dss** is larger than those of the natural purine bases, and thus, **Dss** efficiently excludes the pairing with the natural bases. In contrast, **Pn** and **Px** have a five membered heterocycle, which is smaller than that of the six membered pyrimidines, to fit well with **Dss**. In addition, **Pn** and **Px** efficiently prevent the mispairing with the natural purine bases, due to the electrostatic repulsion between the oxygen atoms of the 2-nitro groups of **Pn** and **Px** and the 1-nitrogens of A and G.^{16,27} In particular, the **Dss**–**Px** pair exhibits very high selectivity in PCR amplification, and the selectivity is similar to that of our previously reported **Ds**–**Px** pair.¹⁶ DNA fragments containing the **Ds**–**Px** pair can be amplified 10⁷–10⁸-fold by 30–40 PCR cycles, with less than a 1% total mutation rate of the unnatural base pair site. As compared to the **Ds**–**Px** pair system, decreasing the substrate concentration of **Dss**, as well as that of **Px**, is better for high fidelity PCR amplification. This is because the misincorporation of **Dss** opposite the natural bases is higher than that of **Ds**, and the

high **dDssTP** concentration inhibits the following polymerase reaction after the **Dss** incorporation opposite **Px**.

The strong fluorescence of **Dss** is visibly diminished by contact quenching with **Pn** or **Px**, but only when **Dss** pairs with **Pn** or **Px** in a duplex, and thus, these fluorophore and quencher base pairs can be used as sensing and diagnostic tools, especially for detecting a target DNA sequence. Here we have shown the applications of the **Dss**–**Pn** pair as a molecular beacon and of the **Dss**–**Px** pair in real-time qPCR. In the molecular beacon incorporating the **Dss**–**Pn** pair into its stem region, the **Dss** fluorescence on–off switching was recognizable with the naked eye, depending on the presence of its target DNA molecule. The 2-nitropyrrole moiety is not stable under basic conditions, and 50% of the 2′-deoxyribonucleoside of **Pn** was decomposed in concentrated ammonia at 55 °C for 4 h.²⁷ Thus, the chemical synthesis of DNA molecular beacons containing the **Ds**–**Pn** pair requires the amidite reagents of the natural bases with labile amino protecting groups, and the deprotection of the synthesized oligomers was performed in concentrated ammonia at room temperature within 3 h.²⁷ Although the quenching ability of **Px** is higher than that of **Pn**, the nucleoside of **Px** is less stable and not suitable for DNA chemical synthesis.

A real-time PCR method was developed, by using a primer containing **Dss** and the **Px** substrate, in which the **Dss** fluorescence was reduced during PCR amplification by incorporating the **Px** substrate opposite **Dss** in the primer. This method is similar to another real-time qPCR method, Plexor, which uses the unnatural base pair between isoguanine (iG) and isocytidine (iC).⁶ The Plexor system involving the iG–iC pair requires a PCR primer containing iC and a fluorophore-linked natural base,

as well as a quencher-linked iG substrate, and thus, it is more complicated than the **Dss**–**Px** qPCR system. The **Dss**–**Pn** pair would also be applicable to other real-time PCR methods, such as those employing Scorpion primers and TaqMan probes.

In this report, we have described the strong quenching ability of 2-nitropyrrole. As shown with the **Px** base, modifications at position 4 of 2-nitropyrrole with unsaturated groups increased the quenching ability. Therefore, in addition to the fluorophore and quencher base pair, the 2-nitropyrrole moiety could be useful as a scaffold to generate new quencher molecules.

Experimental Section

General. DNA fragments containing **Pn** were synthesized with an Applied Biosystems 392 DNA synthesizer, using ultramild CE phosphoramidite reagents for the natural bases (Glen Research). The syntheses of the **Dss** and **Pn** amidite reagents and the triphosphates of **Dss** and $\text{NH}_2\text{-hx-Px}$ have been described previously^{16,19} and the **Px** nucleoside synthesis is described in the Supporting Information. DNA fragments were purified by C18-HPLC with an analytical column (CAPCELL PAK C18 MGIII, 250 mm \times 4.6 mm, Shiseido) or by gel electrophoresis. The fluorescence and UV–vis spectra were obtained on a JASCO FP-6500 spectrofluorometer equipped with a temperature controller (ETC-273T) and on a Beckman DU-530 or DU-650 spectrometer, respectively. UV-monitored thermal denaturation experiments were performed on a SHIMADZU UV-2450 spectrometer equipped with a temperature controller (TMSPC-8).

Fluorescence Quenching Experiments. **dDssTP** (5 μL , 105 μM) was mixed with **dPnTP** (100 μL , 2 mM, 1 mM, 0.5 mM, 0.2 mM, 0.1 mM, and 0.05 mM), **dATP**, **dGTP**, **dCTP**, or **dTTP** (100 μL , 15 mM, 12 mM, 9 mM, 6 mM, 3 mM, and 1 mM) in Tm buffer (10 mM sodium phosphate (pH 7.0), 100 mM NaCl, and 0.1 mM EDTA). Steady-state fluorescence emission spectra of **dDssTP** (5 μM) upon the addition of **dPnTP**, **dATP**, **dGTP**, **dCTP**, or **dTTP** were monitored at the excitation wavelength of 370 nm at 20 $^\circ\text{C}$. The steady-state fluorescence quenching ability was determined by following the Stern–Volmer equation, $F_0/F_1 = 1 + K_{SV}[Q]$, where F_0 and F_1 are the fluorescence intensities of **dDssTP** in the absence and presence of a quencher (**dPnTP**, **dATP**, **dGTP**, **dCTP**, and **dTTP**), $[Q]$ is the quencher concentration, and K_{SV} is the quenching constant. The K_{SV} values were calculated from the slopes of the Stern–Volmer plots by the least-squares method.

PCR Involving the **Dss–**Px** Pair.** PCR (50 μL) was performed in a reaction buffer (20 mM Tris-HCl (pH 8.8), 10 mM KCl, 10 mM $(\text{NH}_4)_2\text{SO}_4$, 2 mM MgSO_4 , and 0.1% Triton X-100) with 10–50 μM $\text{NH}_2\text{-hx-dPxTP}$, 25 or 50 μM **dDssTP**, 0.5 mM each natural dNTP, 1 μM Fwd-primer (40-mer, 5'-CGTTGTAAAACGACGCCAGGATAATCAGACTCACTATAG-3'), 1 μM Rev-primer (24-mer, 5'-TTTCACACAGGAAACAGCTATGAC-3'), and 0.5 nM single-stranded DNA template (55-mer, **Ds**: 5'-TTTCACACAGGAAACAGCTATGACGGCCDStTGGCCCTATAGTGAGTCGTATTATC-3' or Control: 5'-TTTCACACAGGAAACAGCTATGACGGATCCATTCCTATAGTGAGTCGTATTATC-3', the primer regions are underlined) and DeepVent DNA polymerase (0.02 U/ μL , New England Biolabs). The PCR protocol was as follows: 94 $^\circ\text{C}$, 0.5 min; 45 $^\circ\text{C}$, 0.5 min; 65 $^\circ\text{C}$, 4 min. After 15 cycles of PCR, the amplified products in a 7.5 μL aliquot of the reaction mixture were analyzed by denaturing 15% PAGE, and the DNA fragments on the gel were stained with SYBR Green II. The fluorescent bands of the DNA fragments on the gel were detected and quantified with a bioimaging analyzer, LAS-4000 (FUJIFILM), in the DAPI-mode (for **Dss**, exposure time: 5 s) or the SYBR-mode (for DNA). A chemically synthesized DNA fragment containing one **Dss** (61-mer, 15 pmol) was also loaded on the gel, as a **Dss** fluorescent marker. The full-length products of a 20 μL aliquot of the reaction mixture were purified by electrophoresis on an 8% polyacrylamide gel containing 7 M urea, for DNA sequencing analysis.

DNA Sequencing. The cycle sequencing reaction (10 μL) involving the unnatural base pairs^{16,19,27} was performed with the Cycle Sequencing Mix (4 μL) from the BigDye Terminator v1.1 Cycle Sequencing Kit (Applied Biosystems), using approximately 3.5 ng of the gel-purified PCR products as the template, and 2 pmol of the sequencing primer (20-mer, 5'-CGTTGTAAAACGACGCCAG-3'), in the presence of 0.5 nmol of 4-propynylpyrrole-2-carbaldehyde nucleoside triphosphate, **dPaTP** or **ddPaTP**.¹⁶ After 25 cycles of PCR (96 $^\circ\text{C}$, 10 s; 50 $^\circ\text{C}$, 5 s; 60 $^\circ\text{C}$, 4 min), the residual dye terminators were removed from the reaction with CENTRI-SEP columns (Princeton Separations), and the solutions were dried. The residues were resuspended in a formamide solution (3 μL) and were fractionated on the ABI 377 DNA sequencer, using a 6% polyacrylamide gel containing 6 M urea. The sequence data were analyzed with the Applied Biosystems PRISM sequencing analysis v3.2 software.

Hybridization Analysis of Molecular Beacons. To obtain an image with a digital camera, a 50 μL portion of a 2 μM solution of a molecular beacon (MB-C, 26-mer, 5'-ACGCDssCGGGGATTCCTCTATGPnGCGT-3'), dissolved in Tm buffer, was mixed with 50 μL of a 2 μM solution of a perfectly matched target DNA (71G, 71-mer, 5'-ATTGAGCCATACGGACCATGGCTTCATAAATAGAGGAATCCCCGTGTGGGTGGTATTTACCCATGACATCC-3'), dissolved in Tm buffer, in 0.2-ml thin wall tubes. The solutions were heated at 90 $^\circ\text{C}$ for 10 s, and slowly cooled to 25 $^\circ\text{C}$. The image was then obtained under 365-nm UV irradiation at room temperature. For detecting either a perfect target or an imperfect target with a single nucleotide mismatch, a 50 μL portion of a 500 nM solution of a 26-mer molecular beacon, either MB-C or MB-T (5'-ACGCDssCGGGGATTTCTCTATGPnGCGT-3'), was mixed with 12.5 μL of different concentrations of 71-mer target DNA solutions, either 71G or 71A (5'-ATTGAGCCATACGGACCATGGCTTCATAAATAGAGAAATCCCCGTGTGGGTGGTATTTACCCATGACATCC-3'), where the single nucleotide differences are underlined. The solution was incubated at 45 $^\circ\text{C}$ for more than 5 min, and the fluorescence intensity of the solution was measured on a JASCO FP-6500 spectrofluorometer at 45 $^\circ\text{C}$, with excitation and emission wavelengths of 390 and 454 nm, respectively. The fluorescence intensities were normalized by dividing them by the intensity of each molecular beacon without targets.

Real-Time PCR Involving the **Dss–**Px** Pair.** The PCR reaction (25 μL) was performed in 1 \times Titanium Taq buffer (Clontech) with 0.2 mM each natural dNTP, 2 μM $\text{NH}_2\text{-hx-dPxTP}$, 1 μM Primer 1 (29-mer, 5'-AATAATGCDssTCCTCAAAGGTGGTGACTTC-3') and 1 μM Primer 2 (25-mer, 5'-CATGTAGATGCATCAAAGAAGCTC-3'), 1 \times Titanium Taq polymerase (Clontech), different concentrations of 98-bp double-stranded template (final concentrations: 2 fM, 1 fM, 0.2 fM, 0.1 fM, 20 aM, 10 aM, 2 aM, 1 aM, and 0.2 aM) on an Mx3005P system (Stratagene). PCR cycling parameters were 95 $^\circ\text{C}$ for 2 min, followed by 55 cycles of 5 s at 95 $^\circ\text{C}$; and 40 s at 68 $^\circ\text{C}$. The excitation and emission filter set used for the **Dss** fluorescence detection was ALEXA Fluor 350 (350–440 nm), and the raw data were collected by the MxPro qPCR software, ver. 4.10. Graphical representations and analyses of the data were performed with the Plexor Data Analysis Software (Promega). The 98-bp double-stranded template was prepared by primer extension, using two 60-mer chemically synthesized DNA fragments (5'-CATGTAGATGCCATCAAGAGCTCTGAGCCTCCTAAATgacatgcgtgctctggagaac-3' and 5'-TCCTCAAAGGTGGTGACTTCTACGTCTTCGTACGTCTTCGTTCTTTTCgttccagagcacgcatgca-3', the complementary regions are shown in lower case). The primer extension (300 μL) was performed in a reaction buffer (10 mM Tris-HCl, pH 7.5, 7 mM MgCl_2 , and 0.1 mM DTT) with 0.6 mM natural dNTPs, 3 μM each DNA fragment and the exonuclease-proficient Klenow fragment (6 U, TaKaRa), at 37 $^\circ\text{C}$ for 30 min. The products were collected by ethanol precipitation, and the full-length products were purified by electrophoresis on a 10% polyacrylamide gel containing 7 M urea.

Acknowledgment. This work was supported by the Targeted Proteins Research Program and the RIKEN Structural Genomics/Proteomics Initiative, the National Project on Protein Structural and Functional Analyses, Ministry of Education, Culture, Sports, Science and Technology of Japan, and by Grants-in-Aid for Scientific Research (KAKENHI 19201046 to I.H., 20710176 to M.K.) from the Ministry of Education, Culture, Sports, Science and Technology of Japan.

Supporting Information Available: The synthesis and characterization of the **Px** nucleoside; and the quenching of the **Dss** fluorescence by nitropyrrole nucleoside derivatives. This material is available free of charge via the Internet at <http://pubs.acs.org>.

JA1072383